Title

Crossed cerebellar diaschisis on 18F-FDG PET: Frequency across neurodegenerative syndromes and association with 11C-PIB and 18F-Flortaucipir

Journal

Cerebrovascular and Brain Metabolism Reviews, 41(9)

ISSN

1040-8827

Authors

Provost, Karine
La Joie, Renaud
Strom, Amelia
et al.

Publication Date

2021-09-01

DOI

10.1177/0271678x211001216

Peer reviewed

Original Article

JCBFM

Journal of Cerebral Blood Flow & Metabolism
2021, Vol. 41(9) 2329–2343

DOI: 10.1177/0271678X211001216
journals.sagepub.com/home/jcbfm
SAGE

Crossed cerebellar diaschisis on ^{18}F-FDG PET: Frequency across neurodegenerative syndromes and association with ^{11}C-PIB and ^{18}F-Flortaucipir

Karine Provost[1]*, Renaud La Joie[1,*], Amelia Strom[1], Leonardo Iaccarino[1], Lauren Edwards[1], Taylor J Mellinger[1], Julie Pham[1], Suzanne L Baker[2], Bruce L Miller[1], William J Jagust[2,3] and Gil D Rabinovici[1,2,3,4]

Abstract

We used ^{18}F-FDG-PET to investigate the frequency of crossed cerebellar diaschisis (CCD) in 197 patients with various syndromes associated with neurodegenerative diseases. In a subset of 117 patients, we studied relationships between CCD and cortical asymmetry of Alzheimer's pathology (β-amyloid (^{11}C-PIB) and tau (^{18}F-Flortaucipir)). PET images were processed using MRIs to derive parametric SUVR images and define regions of interest. Indices of asymmetry were calculated in the cerebral cortex, basal ganglia and cerebellar cortex. Across all patients, cerebellar ^{18}F-FDG asymmetry was associated with reverse asymmetry of ^{18}F-FDG in the cerebral cortex (especially frontal and parietal areas) and basal ganglia. Based on our operational definition (cerebellar asymmetry $>$3% with contralateral supratentorial hypometabolism), significant CCD was present in 47/197 (24%) patients and was most frequent in corticobasal syndrome and semantic and logopenic variants of primary progressive aphasia. In β-amyloid-positive patients, mediation analyses showed that ^{18}F-Flortaucipir cortical asymmetry was associated with cerebellar ^{18}F-FDG asymmetry, but that cortical ^{18}F-FDG asymmetry mediated this relationship. Analysis of ^{18}F-FDG-SUVR values suggested that CCD might also occur in the absence of frank cerebellar ^{18}F-FDG asymmetry due to symmetrical supratentorial degeneration resulting in a bilateral diaschisis process.

Keywords

Alzheimer's, diaschisis, FDG, PET, Tau

Received 8 February 2021; Revised 8 February 2021; Accepted 15 February 2021

Introduction

Crossed cerebellar diaschisis (CCD), defined as a decrease in hemispheric cerebellar perfusion or metabolism contralateral to a supratentorial lesion, was described nearly forty years ago on positron emission tomography (PET) by Baron et al.[1,2] This phenomenon is thought to be due to neuronal deactivation secondary to damage to glutamatergic excitatory neurons in the cortico-ponto-cerebellar tracts.[3–6] A large body of literature has studied cerebellar diaschisis in patients with stroke[2,3,7–11] and other conditions such as epilepsy,[12–15] encephalitis,[16–18] head trauma,[19] and malignant brain lesions.[20–24] However, in spite of CCD being, in

[1]Memory and Aging Center, Department of Neurology, Weill Institute for Neurosciences, University of California San Francisco, San Francisco, CA, USA
[2]Lawrence Berkeley National Laboratory, Berkeley, USA
[3]Helen Wills Neuroscience Institute, University of California Berkeley, Berkeley, CA, USA
[4]Department of Radiology and Biomedical Imaging, University of California San Francisco, San Francisco, CA, USA

*These authors contributed equally to this article.

Corresponding author:
Karine Provost, Memory and Aging Center, University of California San Francisco, 675 Nelson Rising Lane, Suite 190, San Francisco, CA 94143, USA.
Email: provost.karine@gmail.com

our experience, a common incidental finding upon visual assessment of ^{18}F-Fluorodeoxyglucose (FDG) brain PET studies, reports in patients with neurodegenerative diseases are limited.[25–29] Recently, in a case series of four patients with Alzheimer's disease (AD), Reesink et al. found no relationship between the accumulation of β-amyloid on ^{11}C-Pittsburgh compound B (PIB) and contralateral cerebellar hypometabolism on ^{18}F-FDG, suggesting that CCD is a β-amyloid-independent process.[25] The relationship between CCD and pathologic aggregation of tau measured in vivo using ^{18}F-Flortaucipir PET[30] has never been investigated. Based on the known relationship between ^{18}F-Flortaucipir signal and local neurodegeneration[31–39] in AD, we hypothesized that cortical asymmetry of ^{18}F-Flortaucipir will be associated with the presence of contralateral cerebellar hypometabolism on ^{18}F-FDG in β-amyloid positive subjects. We also hypothesized that CCD would be more frequent in clinical syndromes that are typically associated with asymmetric presentations and neurodegeneration, such as corticobasal syndrome (CBS),[40] semantic variant primary progressive aphasia (svPPA)[41] and logopenic variant primary progressive aphasia (lvPPA).[41,42] Finally, while there have been some reports of CCD as a potential prognostic biomarker in stroke and in tumors,[43–46] the clinical significance of this finding in neurodegenerative syndromes remains unknown.

The objectives of this study were to (1) assess the prevalence of CCD in a large cohort of cognitively impaired patients with suspected neurodegenerative diseases and across different clinical diagnoses; (2) to investigate the relationship between CCD and cortical asymmetries of glucose metabolism (^{18}F-FDG), β-amyloid deposition (^{11}C-PIB) and tau burden (^{18}F-Flortaucipir) on brain PET studies; and (3) to evaluate the correlation between CCD and measures of clinical disease severity.

Materials and methods

Study design and participants

We retrospectively included 197 consecutive patients enrolled in research studies at the Memory and Aging Center, University of California San Francisco (UCSF), who had undergone ^{18}F-FDG PET between 2012 and 2019 on the same PET/CT scanner, and had structural MRI available. Patients underwent a complete clinical evaluation including a structured caregiver interview, neuropsychological and neurological assessment (described in detail elsewhere[31,47]) Tests of cerebellar function were performed for most patients and assessed by retrospective chart review, including assessment of tremor in the upper and lower limbs, pronation-supination test, finger-to-nose test, heel-to-shin test, tandem walk and assessment for ataxic gait. Clinical diagnosis was based on consensus research criteria following multi-disciplinary evaluation, blinded to biomarker results. In short, patients were assigned a diagnosis of mild cognitive impairment,[48] dementia due to Alzheimer's disease,[49] behavioral variant frontotemporal dementia,[50] variants of primary progressive aphasia,[51] corticobasal syndrome[52] or progressive supranuclear palsy.[53] Patients who did not meet criteria for these diagnoses were assigned "other" (detailed in Table 1).

Table 1. Patient characteristics.

	HC (n = 76)	Patients (n = 197)
Age (y)	67 ± 14 [22-90]	64 ± 9 [32-95]
Sex (n_{male}, %)	30 (39%)	106 (54%)
Education	16 ± 2 [12-20]	17 ± 3 [5-28]
MMSE	29 ± 1 [26-30]	23 ± 6 [0-30]
CDR-SB	n/a	4.0 ± 2.7 [0-15]
^{11}C-PiB-PET positive	19/56	110/197
Clinical diagnosis		
MCI		38
tAD		56
PCA		19
lvPPA		14
bvFTD		23
nfvPPA		14
CBS		11
svPPA		7
PSP		6
Other†		9

Note: For continuous variables, mean ± SD [min-max] are shown. MMSE: Mini-mental status exam; CDR-SB: Clinical dementia rating scale sum of boxes; HC: healthy controls; MCI: mild cognitive impairment; tAD: Alzheimer's disease dementia (typical); PCA: posterior cortical atrophy; lvPPA: logopenic variant primary progressive aphasia; bvFTD: behavioral variant frontotemporal degeneration; nfvPPA: non-fluent variant primary progressive aphasia; CBS: corticobasal syndrome; svPPA: semantic variant primary progressive aphasia; PSP: progressive supranuclear palsy.

†Other: 5 with traumatic brain injury/chronic traumatic encephalopathy syndrome, 2 with no specific diagnosis, one with bipolar disorder and cognitive impairment not meeting criteria for neurodegenerative syndrome, one with Parkinson's disease with cognitive impairment.

We also retrospectively included 76 cognitively unimpaired controls from the Berkeley Aging Cohort Study (BACS) who underwent ^{18}F-FDG PET on the same scanner as patients and had structural MRI available. Controls were recruited by advertisement from the community, endorsed no significant cognitive problems, and scored within the normal range on a battery of neuropsychological tests.[54]

Written informed consent was obtained from all subjects or their surrogates. The study was approved

by the University of California San Francisco, University of California Berkeley and Lawrence Berkeley National Laboratory institutional review boards for human research. All procedures performed were in accordance with the ethical standards of the institutional research committee and with the 1975 Helsinki declaration and its later amendments.

PET acquisition

All patients and controls underwent ^{18}F-FDG brain PET (~5–10 mCi dose, acquired at 30–60 minutes post-injection) on a Siemens Biograph 6 Truepoint PET/CT (Siemens, Erlangen, Germany) at the Lawrence Berkeley National Laboratory in 3 D acquisition mode. 117 patients also underwent scanning with ^{11}C-PIB (~15 mCi, minimum of four 5-min frames acquired at 50–70 minutes post-injection) and ^{18}F-Flortaucipir (~10 mCi, minimum of four 5-min frames acquired at 80–100 minutes post-injection) on the same scanner. Mean intervals between scans are shown in Supplementary Table 1. For all brain PET studies, a low-dose CT was performed for attenuation correction. PET data were reconstructed using an ordered subset expectation maximization algorithm and smoothed with a 4-mm Gaussian kernel with scatter correction. All subjects also underwent MRI (T1-weighted MRI sequence, on a 3-T Siemens Tim Trio (n = 127) or a 3-T Siemens Prisma FIT (n = 70) scanner for patients, and on a 3-T Siemens Tim Trio (n = 29) or a 1.5-T Siemens Magnetom Avanto (n = 47) for controls (Siemens, Erlangen, Germany)). Detailed acquisition parameters are described elsewhere.[34,55] MRI was used for PET processing only.

PET processing

All the PET data presented in this paper are based on tissue-to-reference ratio values. PET images were co-registered to corresponding T1-weighted MRIs in native space. Each subject's MRI was segmented using FreeSurfer version 5.3 (https://surfer.nmr.mgh.harvard.edu/) to define regions of interest. PET SUVR images were generated using tracer specific reference regions (pons for ^{18}F-FDG, cerebellar gray matter for ^{11}C-PIB, and inferior cerebellar gray matter for ^{18}F-Flortaucipir, as detailed elsewhere[34,54,56]) Non-partial volume corrected data were used.

For all three radiotracers, SUVR values were extracted from each FreeSurfer-derived ROI and aggregated into large left and right composite regions using a size-weighted average: cerebral cortex (all cortical areas), cerebellar cortex, and basal ganglia (composite of caudate, putamen and globus pallidus). Inferior cerebellar gray matter was used instead of full cerebellar cortex for ^{11}C-PIB and ^{18}F-Flortaucipir to avoid spillover from supratentorial signal. To analyze the relationship between CCD and cerebral cortex asymmetries in more detail, we also extracted left and right SUVRs for composite regions representing the frontal, parietal, temporal and occipital lobes.

For each tracer and composite region, indices of asymmetry (IA) were calculated using the formula: *(right SUVR – left SUVR)/bilateral SUVR*.[22,57] As such, a positive IA in the cerebral cortex on ^{18}F-FDG corresponds to more severe hypometabolism in the left hemisphere, whereas a positive IA in the cerebral cortex on ^{11}C-PIB/^{18}F-Flortaucipir indicates greater β-amyloid/tau burden in the right hemisphere. For some analyses (see below), we used the absolute value of IA, reflecting the intensity of asymmetry regardless of laterality.

Definition of β-amyloid (A) and tau (T) status for patients

Based on the AT(N) research framework proposed by Jack et al.[58] to define AD *in vivo* with (imaging and/or fluid) biomarkers, β-amyloid (A) status was defined by independent visual assessment of ^{11}C-PIB.[59] Tau (T) status was defined using the bilateral weighted temporal meta-ROI SUVR threshold of 1.27, as previously described by Ossenkoppele et al.[60]

Operationalization of CCD

Although most of the analyses presented in this manuscript considered ^{18}F-FDG cerebellar asymmetry as a continuous variable using the IA described above, we also aimed to identify patients with significant CCD, i.e. patients with both significant ^{18}F-FDG cerebellar asymmetry and contralateral supratentorial asymmetry. We operationalized this definition as follows. First, we analyzed ^{18}F-FDG asymmetry in the control group to establish the normal range of ^{18}F-FDG IA values for each ROI (cerebellar cortex, basal ganglia, frontal, parietal, temporal, and occipital lobe). The distribution of each region's IA was visually inspected, and scans with extreme IA values were visually checked by a nuclear medicine physician (K.P.), resulting in 2 individuals being excluded from the control group: one had CCD (hypometabolism in the right cerebellar cortex and hypometabolism in the left cerebral hemisphere, Supplementary Figure 1(b), left panel), and another had significant asymmetry in the basal ganglia, likely due to vascular disease (Supplementary Figure 1 (b), right panel). Second, we identified patients with significant ^{18}F-FDG cerebellar asymmetry. A threshold of absolute ^{18}F-FDG cerebellar IA > 3% was used, based on the distribution of values in the 74 healthy

controls: this threshold corresponded to mean + 2 standard deviations (SD) of the distribution of ^{18}F-FDG cerebellar IA in the controls (2.98%), none of which were suprathreshold. Third, we identified patients with significant ^{18}F-FDG asymmetry in at least one supratentorial region using a threshold corresponding to the mean + 2SD of the 74 controls (2% for basal ganglia, 3% for frontal, 5% for parietal, 5% for temporal and 6% for occipital lobe). Last, we considered patients to have significant CCD when we observed both a significant cerebellar IA and a significant but reverse asymmetry in at least one of the supratentorial regions (basal ganglia, frontal, parietal, temporal, or occipital lobe). The presence of CCD was further confirmed by visual assessment.

Statistical analyses

To assess for normality of data, Shapiro-Wilk tests were performed on all variables, in addition to assessing distribution on density plots. Pearson correlations were conducted to assess the relationship between ^{18}F-FDG cerebellar IA and ^{18}F-FDG, ^{11}C-PIB and ^{18}F-Flortaucipir cortical IA, as well as measures of clinical disease severity (Mini-Mental Status Exam (MMSE) and Clinical dementia rating scale – sum of boxes (CDR-SB)). For non-normally distributed variables, nonparametric tests based on ranked data were performed to confirm robustness of the results. Mediation analyses were performed between ^{18}F-FDG cerebellar IA and ^{18}F-Flortaucipir cortical IA, MMSE and CDR-SB, reflecting indirect (i.e. mediated) and direct pathways. A forward procedure for variable selection in a multiple linear regression was used to assess regional ^{18}F-FDG IA (frontal, parietal, temporal, occipital and basal ganglia) as predictors of cerebellar IA. General linear models were used to assess interactions between ^{18}F-FDG cerebellar IA, clinical diagnosis, MMSE and CDR-SB. Note that for all analyses including multi-tracer PET data, we focused on cerebral cortex PET signal and did not consider basal ganglia PET SUVR, due to the intense "off-target binding" observed on ^{18}F-Flortaucipir-PET.[61,62]

Statistical analyses were performed using SPSS (version 25, IBM, Armonk, NY). Jamovi (version 1.20, www.jamovi.org)[63] was used to conduct mediation analyses and general linear models.

Results

Demographics for all subjects are shown in Table 1. Average patient age was 64 years (range 32-95), with a slight male predominance (54%). The vast majority of patients self-identified as White/Caucasian (86%, n = 171). Others were African American (n = 3), Asian (n = 6), Asian Indian (n = 1); 2 patients endorsed multiple categories while 14 did not disclose this information. The patient sample was heterogeneous with clinical diagnoses of mild cognitive impairment, non-AD disorders (see breakdown of clinical diagnoses in Table 1), as well as both typical and atypical variants of AD dementia, including patients meeting diagnostic criteria for logopenic variant primary progressive aphasia (lvPPA)[51] and posterior cortical atrophy syndrome (PCA).[64]

Frequency of CCD across clinical syndromes

Representative cases of CCD in patients with posterior cortical atrophy, corticobasal syndrome (CBS), semantic variant primary progressive aphasia (svPPA), and progressive supranuclear palsy are shown in Figure 1. Significant asymmetry of cerebellar metabolism was present in 51/197 patients (26%). Only four of these 51 subjects did not reach quantitative criteria for CCD (Figure 2(a)) as they showed only minimal supratentorial asymmetry upon visual assessment, therefore possibly representing cases of isolated asymmetry of cerebellar glucose metabolism. The remaining 47 subjects exhibited significant CCD on both quantitative and visual assessment. The highest frequency of CCD was observed in patients with clinical diagnoses of CBS, svPPA, lvPPA, PCA and non-fluent variant primary progressive aphasia, though most diagnostic subgroups were too small to conduct statistical analyses (Figure 2(b)). When grouping clinical diagnoses into typical AD (i.e. amnestic AD and MCI, n = 94), atypical AD (i.e. lvPPA and PCA, n = 33), or non-AD disorders (n = 70), there was a statistically significant difference in ^{18}F-FDG cerebellar IA between diagnostic groups (Kruskal-Wallis H p= .008). Post-hoc pairwise comparisons showed that the ^{18}F-FDG cerebellar IA was significantly higher in the atypical AD group compared to typical AD (Bonferroni corrected p= .007), while differences with the non-AD diagnostic group did not reach statistical significance (Bonferroni corrected p= .33 and p= .26).

Relationships between cerebellar and supratentorial ^{18}F-FDG asymmetry

The distribution of cortical IA for each modality is shown in Supplementary Table 2. ^{18}F-FDG cerebellar IA showed a significant inverse correlation with both ^{18}F-FDG basal ganglia IA ($r = -.617$, $p < .001$) and cortical IA ($r = -.739$, $p < .001$) (Figure 3). This relationship was present in both β-amyloid negative (n = 87; $r = -.567$ for the basal ganglia, $r = -.643$ for the cerebral cortex, both ps $< .001$) and β-amyloid positive subgroups (n = 110; $r = -.654$ for the basal

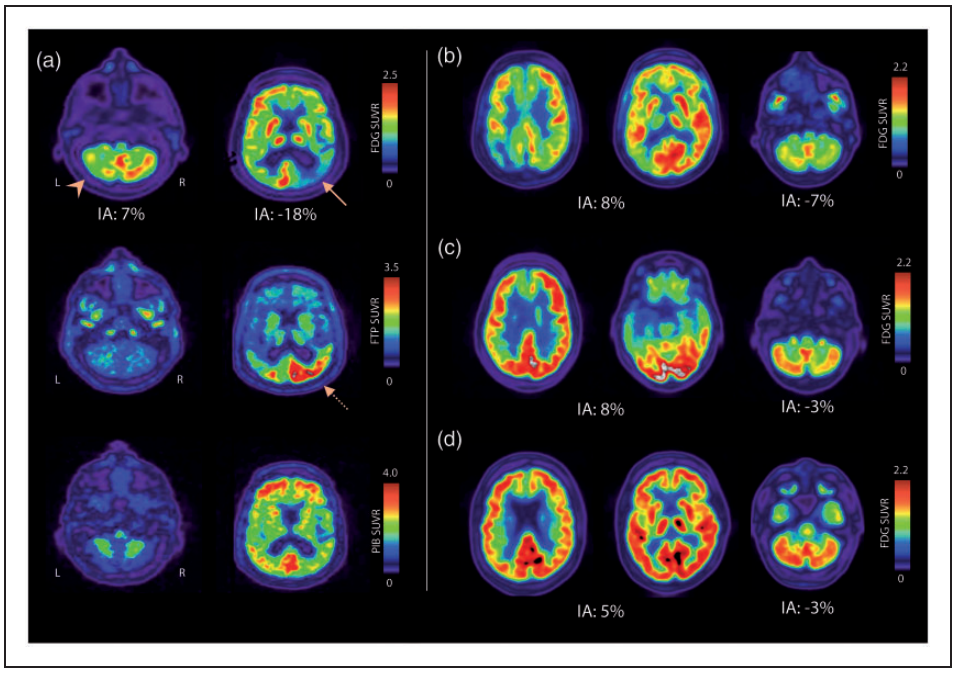

Figure 1. Representative cases of CCD.
(a) 76 year-old AD (A+T+) patient with posterior cortical atrophy syndrome. CCD is noted on ^{18}F-FDG PET (top row), with left cerebellar hypometabolism (arrowhead). Cortical hypometabolism is asymmetric, with predominant involvement of the hemisphere contralateral to cerebellar hypometabolism (arrow). Significant asymmetry is also noted on ^{18}F-Flortaucipir PET (dotted arrow, middle row), with greater binding in the right cerebral cortex mirroring hypometabolism, which is not the case for ^{11}C-PIB (bottom row). The right panel shows selected ^{18}F-FDG axial slices of patients with CCD and clinical diagnoses of corticobasal syndrome (b), semantic variant primary progressive aphasia (c), and progressive supra-nuclear palsy (D, very mild CCD). Cortical and cerebellar indices of asymmetry (IA) are indicated for ^{18}F-FDG.

ganglia, r= -.792 for the cerebral cortex, both ps< .001). Correlations tended to be stronger in the β-amyloid positive group, and this difference was significant for the relationship with the cerebral cortex (based on Fisher r-to-z transformation: $Z = 2.15$, $p = .03$) but not the basal ganglia ($Z = 0.95$, $p = .34$).

To determine whether the relationship was driven solely by subjects with significant cerebellar asymmetry, we analyzed separately subjects with absolute cerebellar IA of less than 3% (n = 146). The relationship between cerebellar IA and cortical IA remained significant ($r = -.566$, p< .001). No significant relationship was found in healthy controls, however (r= .018, p= .88).

When dividing cortical glucose metabolism into lobar (frontal, parietal, temporal, occipital) ROIs, correlation analyses showed that in patients, asymmetry in each lobe was associated with inverse asymmetry in the cerebellum ($rs < -.50$, ps< .001, Supplementary Table 3), while no significant correlation was found in controls. In patients, IA between supratentorial lobes were highly inter-correlated ($rs > .43$, all $ps < .001$, Supplementary Table 3). Accordingly, we ran a stepwise regression model with a forward procedure to select the best predictors of cerebellar ^{18}F-FDG IA. The resulting model accounted for 61.1% of total variance in cerebellar ^{18}F-FDG IA ($F(4,192) = 75.45$, $p < .001$) and included frontal (β= -0.410, p< .001), parietal (β= -0.503, p< .001), temporal ($\beta = 0.243$, p= .01) and basal ganglia (β= -0.147, p= .03) IA as independent predictors.

Relationships between cerebellar ^{18}F-FDG asymmetry and PET imaging of AD pathology

Next, we assessed whether CCD could reflect asymmetry of underlying β-amyloid and tau pathology in AD. We restricted the following analyses to patients with biomarker evidence of AD (A + T+, n = 74)). Regarding β-amyloid, there was no relationship between $^{18-}$F-FDG cerebellar IA and cortical ^{11}C-PIB IA ($r = -.074$, $p = .53$; Spearman's rho= .039, p= .74, Figure 4(a)). Regarding tau, we found that higher cortical ^{18}F-Flortaucipir in one hemisphere was associated with decreased ^{18}F-FDG in the contralateral cerebellum (r= .701, p< .001; Spearman's rho= .664, p< .001,

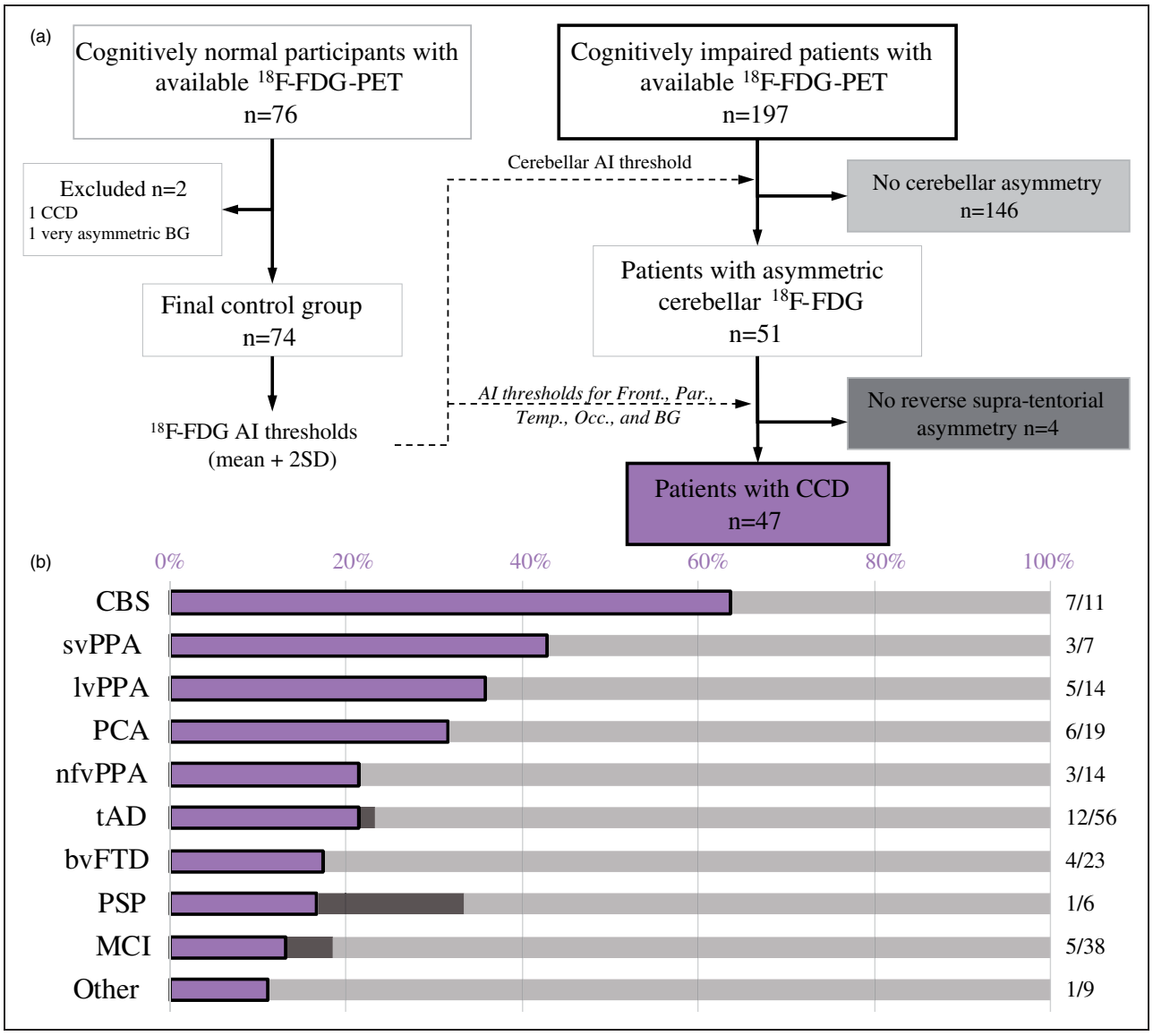

Figure 2. Study workflow and operationalization of crossed cerebellar diaschisis (CCD) (a) and frequency of CCD by clinical diagnosis (b).
BG: basal ganglia; AI: asymmetry index; Front.: frontal; Par.: parietal; Temp.: temporal; Occ.: occipital; CBS: corticobasal syndrome; svPPA: semantic variant primary progressive aphasia; lvPPA: logopenic variant primary progressive aphasia; PCA: posterior cortical atrophy; nfvPPA: non-fluent variant primary progressive aphasia; tAD: Alzheimer's disease dementia (typical); bvFTD: behavioral variant frontotemporal degeneration; PSP: progressive supranuclear palsy; MCI: mild cognitive impairment.

Figure 4(b)). Supratentorial cortical IA of ^{18}F-FDG and ^{18}F-Flortaucipir were also highly correlated (r= -.844, p< .001). Mediation analyses showed that the relationship between ^{18}F-Flortaucipir asymmetry in the cortex and ^{18}F-FDG asymmetry in the cerebellum was highly mediated (79%) by the relationship between ^{18}F-Flortaucipir and ^{18}F-FDG cortical IA (Figure 4(c)).

To ensure that results were not biased by long delay between scans, analyses were replicated in the subgroup of 49 A+T+ patients who underwent ^{18}F-FDG, ^{11}C-PIB, and ^{18}F-Flortaucipir within a month (maximal delay between first and last PET scan = 30 days); all results remained unchanged. Briefly, ^{18}F-FDG cerebellar IA was correlated with ^{18}F-Flortaucipir cortical IA ($r = 0.611$, $p < .001$) but not ^{11}C-PIB IA ($r = -.030$, $p = .84$). ^{18}F-FDG cortical IA was associated with ^{18}F-Flortaucipir cortical IA ($r = -.824$, $p < .001$), and mediated the relationship between ^{18}F-Flortaucipir cortical IA and ^{18}F-FDG cerebellar IA (indirect path: $p < .001$, direct path: $p = .99$, percent mediation = 99.9%).

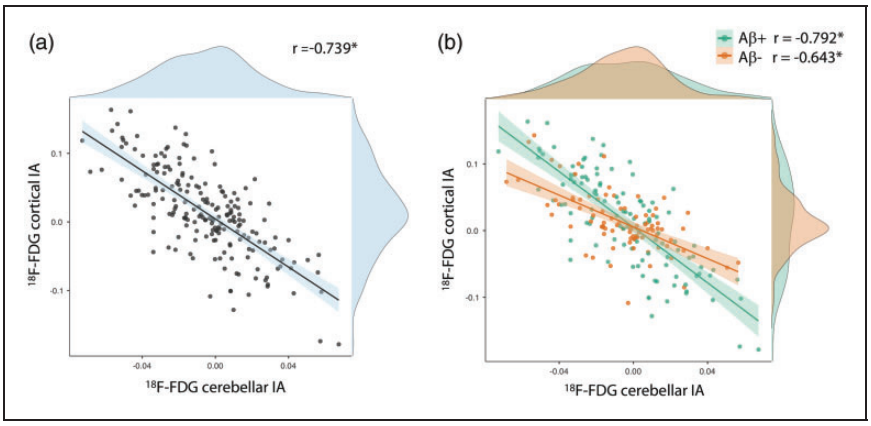

Figure 3. Association between ^{18}F-FDG cortical and cerebellar indices of asymmetry.
(a) in all patients (n = 197), (b) in β-amyloid negative patients (n = 87) and in β-amyloid positive patients (n = 110)
IA: index of asymmetry; r: Pearson correlation coefficient, *p < .001

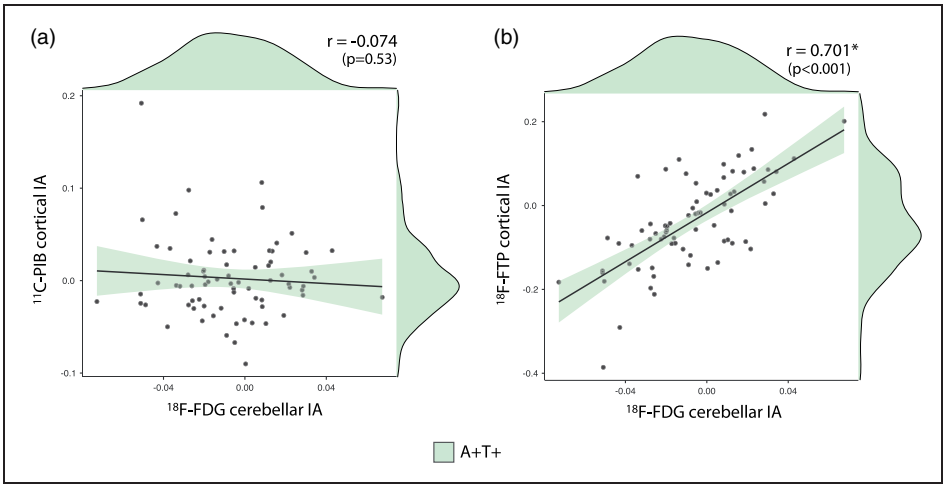

Figure 4. Association between ^{18}F-FDG cerebellar index of asymmetry and cortical index of asymmetry of ^{11}C-PIB (a) and ^{18}F-Flortaucipir (b) Mediation analyses between ^{18}F-FDG cerebellar IA and ^{18}F-Flortaucipir cortical IA (C).
In A+T+ patients (n=74)
IA: index of asymmetry; r: Pearson correlation coefficient.
*indicates statistical significance (p < 0.05)

Since mild to moderate ^{18}F-Flortaucipir signal has occasionally been reported in non-AD neurodegenerative disorders,[55,65,66] we sought to confirm that the relationship observed in A + T+ subjects was specific to Alzheimer's pathology, and not merely reflecting off-target binding of ^{18}F-Flortaucipir to neurodegeneration or other pathology. We confirmed that there was no significant relationship between ^{18}F-Flortaucipir cortical IA and ^{18}F-FDG cerebellar IA in β-amyloid negative subjects (n = 35, r= .230, p= .18).

Lastly, we investigated whether asymmetry in cerebellar metabolism on ^{18}F-FDG was indeed due to diaschisis from supratentorial areas, rather than local cerebellar amyloid or tau pathology, by analyzing the relationships between the cerebellar IA of ^{18}F-FDG, ^{18}F-Flortaucipir and ^{11}C-PIB in the 74 A + T+ subjects. No significant relationship was found for ^{11}C-PIB (r= .077, p= .51) or for ^{18}F-Flortaucipir (r= -.202, p= .09).

Relationship between CCD, clinical disease severity and cerebellar function

We investigated whether there was a correlation between the presence of significant asymmetry in cerebellar glucose metabolism on ^{18}F-FDG, and measures

of clinical disease severity (MMSE and CDR-SB). In the whole cohort (n = 197), there was a weak negative correlation between absolute ^{18}F-FDG cerebellar IA and MMSE score (r= -.260, p< .001, r^2= .067; Spearman's rho= -.214, p = 0.003) and a weak positive correlation with CDR-SB (r= .152, p= .04, r^2= .023; Spearman's rho= .236, p = 0.001). These associations remained significant in models taking into account clinical diagnosis (typical AD, atypical AD, non-AD); no MMSE*diagnosis or CDR*diagnosis interaction was significant (Supplementary Figure 2). These results provide evidence that ^{18}F-FDG cerebellar asymmetry is higher in more severely impaired patients across diagnostic groups (Figure 5). Mediation analyses revealed that for both MMSE and CDR-SB, greater disease severity explained more asymmetric cortical hypometabolism, which in turn was associated with more asymmetric cerebellar ^{18}F-FDG signal (Supplementary Figure 3). In contrast to measures of clinical severity, demographics such as age (r= .106, p= .14), sex (t = 0.46, p= .65) or education (r= -.030, p= .68) were not significantly associated with ^{18}F-FDG cerebellar IA.

Finally, we assessed whether there was a difference in tests of cerebellar function on neurological examination in subjects with and without CCD. Details of physical examination findings can be found in Supplementary Table 4. There was no statistically significant difference in any of the cerebellar function tests between the two groups. Furthermore, the vast majority of patients with CCD did not display signs of cerebellar dysfunction on physical examination. Of the few patients who did exhibit asymmetric signs on neurological examination, they tended to be isolated and were most likely due to severe supratentorial neurodegeneration (e.g.: isolated impairment in right limb supination/pronation in a patient with left hemisphere predominant corticobasal degeneration).

Beyond asymmetry: Bilateral CCD?

While all aforementioned analyses were based on the assessment of cerebellar and supratentorial PET asymmetries, consistent with the CCD literature in focal lesions, the neurodegenerative diseases included in the present study usually affect both cerebral hemispheres with various degrees of asymmetry. It is therefore possible that a "double CCD" phenomenon could occur in patients with bilateral cerebral degeneration: in such cases, glucose metabolism would be decreased in both cerebellar hemispheres without significant asymmetry. To test this hypothesis, we analyzed cerebellar and cerebral ^{18}F-FDG SUVR values (using the pons as a reference region) rather than IA values in the group of 146 patients with no cerebellar asymmetry, i.e. an absolute ^{18}F-FDG cerebellar IA of less than 3% (see Figure 2).

When comparing these patients (n = 146) to the control group (n = 74), we observed a major decrease in cerebral ^{18}F-FDG SUVR (t = 6.38, p<.001 in an analysis of covariance controlling for age), and a mild decrease of cerebellar ^{18}F-FDG SUVR (t = 2.36, p=.02) (Figure 6(a)). In patients, cerebellar and cerebral ^{18}F-FDG SUVR values were correlated (r=.510, p<.001). When hemispheres were considered separately, all four ^{18}F-FDG SUVR values were intercorrelated (all rs $\geq$ .467, ps < .001) but correlations between cerebral and cerebellar SUVRs were stronger when assessed contra-laterally (e.g. left cerebral cortex and

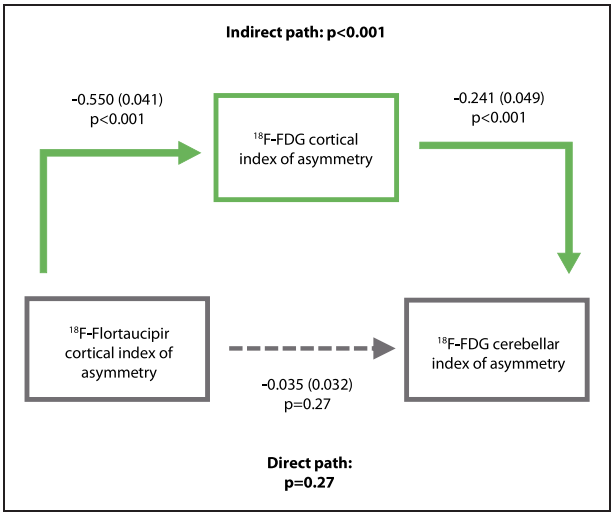

Figure 5. Relationship between ^{18}F-FDG cerebellar IA, MMSE (a) and CDR-SB (B), n = 197.
*indicates statistical significance (p < 0.05)

right cerebellum: r= .506) rather than ipsi-laterally (e.g. left cerebral cortex and left cerebellum, r= .467; Fisher r-to-z transformation: $Z = 2.36$, $p = 0.02$; Figure 6(b)). Finally, multiple regression analyses were run separately to explain left and right cerebellar ^{18}F-FDG SUVR using both left and right cerebral cortex ^{18}F-FDG SUVR. In both models, the best predictor for cerebellar SUVR was the contralateral cerebral cortex SUVR ($p = 0.002$ for the left cerebellum SUVR model, $p = 0.068$ for the right cerebellum SUVR model, see Figure 6(c)).

Results were comparable, although more strongly significant, when considering all 197 patients instead of the subsample with symmetrical cerebellar ^{18}F-FDG signal (Supplementary Figure 4).

Discussion

Our results provide novel insight on the phenomenon of CCD in neurodegenerative diseases. CCD, defined as a left/right asymmetry in cerebellar ^{18}F-FDG signal in the presence of reverse supratentorial asymmetry, was relatively frequent in our patient sample, especially in patients with more severe dementia severity. There was an association between cerebellar asymmetry of glucose metabolism, cortical asymmetries of ^{18}F-FDG and ^{18}F-Flortaucipir, but not ^{11}C-PIB. Data also suggested that a bilateral CCD process might occur in patients without significant cerebellar ^{18}F-FDG asymmetry, consistent with the bilateral involvement of supratentorial areas in most neurodegenerative diseases included in our cohort.

The prevalence of (asymmetric) CCD in our cohort, as defined by thresholds derived from normative ^{18}F-FDG asymmetry in cognitively unimpaired older adults, was relatively high. Twenty-six percent of patients were found to have absolute cerebellar IA greater than 3%, and the vast majority (92%) of those also met our operational definition of CCD (i.e. asymmetry in cerebellar metabolism with contralateral asymmetry in supratentorial glucose metabolism) as confirmed by quantitative and visual assessment. In comparison, a higher prevalence of CCD has been reported in patients with other conditions. The prevalence of CCD with stroke was reported to be as high as 50% on perfusion SPECT by Kim et al.,[8] 58% on $^{15}O_2$ PET oxygen consumption[3] and as high as 40% in patients with head trauma on ^{18}F-FDG PET by Alavi et al.[19] The operational definition of CCD differs from study to study, however, and the results aren't directly comparable. The fact that stroke and head trauma tend to be relatively focal and often unilateral while neurodegenerative diseases are usually more widespread may also in part explain the difference in prevalence between these conditions. In spite of this, the relatively high prevalence in our population suggests that the phenomenon of CCD is under-reported and understudied in neurodegenerative syndromes. Interestingly, we found that the frequency of CCD was higher in specific clinical phenotypes, particularly in typically asymmetric presentations such as svPPA, CBS and nfvPPA. Patients with atypical presentations of AD (lvPPA and PCA syndromes) also had a higher frequency of CCD compared to the typical amnestic presentation. It is known that hypometabolism and tau pathology are often asymmetric in the cortex of atypical AD patients[32,55,67–69]; therefore, it is unsurprising that these phenotypes would be associated with a higher frequency of CCD in our data.

The significant inverse relationship between cortical and cerebellar IA on ^{18}F-FDG is in line with the pathophysiologic mechanism of CCD, i.e. a supratentorial lesion causing downstream hypometabolism in the contralateral cerebellum.[1,2] One interesting finding in our cohort was the presence of this relationship even in patients with subthreshold asymmetry in cerebellar metabolism, while no significant relationship was found in the control group. This suggests that CCD is a continuum, and patients with neurodegenerative diseases may have subtle manifestations of diaschisis even before it is perceptible on visual assessment.

Our analyses of patients without notable cerebellar ^{18}F-FDG asymmetry showed that, at the group level, patients had decreased ^{18}F-FDG SUVR values in the cerebellum compared to controls. In addition, ^{18}F-FDG SUVR values within each cerebellar hemisphere were more strongly correlated with ^{18}F-FDG SUVR in the contralateral, rather than ipsilateral cerebral hemisphere. Altogether, these data suggest that bilateral CCD might occur in some patients and that a definition of CCD purely based on left/right asymmetries, in line with the literature on focal supratentorial lesions, might lack sensitivity in the context of neurodegenerative diseases that most often affect both hemispheres.

In stroke, it has been proposed that lesions localized in the frontal lobes or thalamus are associated with CCD,[7,22,70,71] while temporal lesions alone did not seem to be associated with this phenomenon.[3] Lesions caused by malignant brain tumors localized in the frontal lobe were also found to be associated with CCD.[21] Mechanistically, these observations are consistent with the fact that the densest cortico-ponto-cerebellar projections arise from the frontal lobes.[72] In our cohort, metabolic asymmetry in the frontal and parietal lobes was most strongly associated with cerebellar asymmetry on ^{18}F-FDG. Furthermore, results of our multivariate regression model show that, though ^{18}F-FDG asymmetry in the frontal, parietal, temporal and basal ganglia regions were all significant predictors of asymmetry in cerebellar glucose

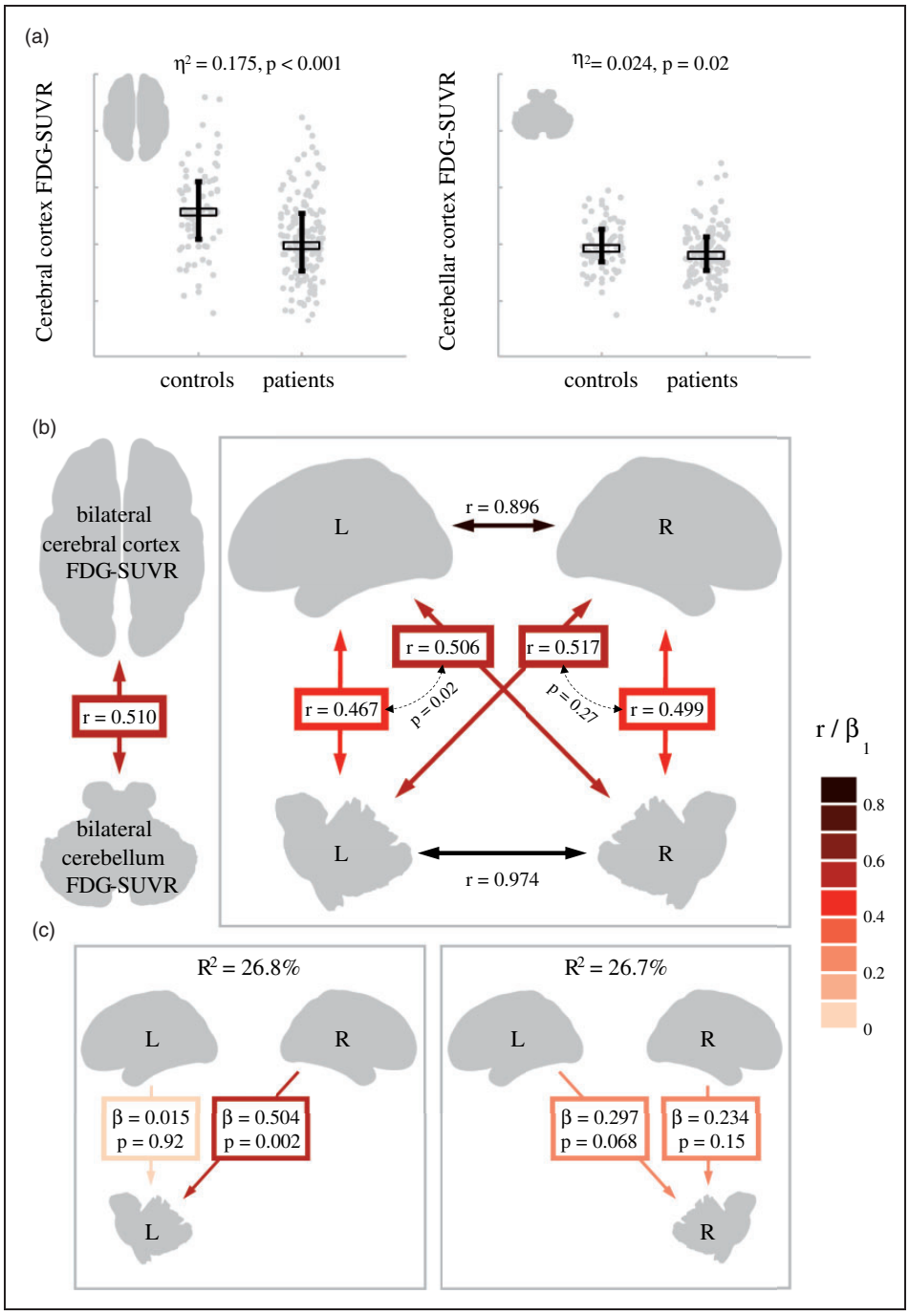

Figure 6. Relationships between cerebral and cerebellar cortex ^{18}F-FDG-SUVR values in patients without significant cerebellar asymmetry.

a. Patients (n=146) versus controls (n = 74) ^{18}F-FDG-SUVR comparisons in the whole cerebral and cerebellar cortices. All SUVR values are calculated using the pons as a reference region. Statistical comparisons include age as a covariate. Plots show individual values, medians (thick horizontal line) and interquartile ranges (vertical whiskers).

b. Bivariate associations between cerebral and cerebellar SUVRs in patients. Thick colored double-headed arrows indicate bivariate correlation coefficients; smaller dashed arrows represent the statistical comparison between two dependent correlations based on Fished r-to-z transformation.

c. Multiple regression models conducted in the patient group to assess the relative contribution of Left/Right cerebral cortex ^{18}F-FDG-SUVR to each cerebellar hemisphere ^{18}F-FDG-SUVR. β values are standardized regression estimates.

metabolism, cortical asymmetry in the frontal lobes alone explained 55% of the variance (r= -0.743). Of note, the inverse calculated β value for the temporal lobe in the multivariate model may be due to collinearity between all predictors in the model, given that a strong negative correlation was found between ^{18}F-FDG IA in the temporal cortex and cerebellum in the pairwise correlations (Supplementary Table 3). Our results are consistent with previously described findings in a small sample of 26 AD patients, which found significant regional correlations between cerebellar and cortical asymmetry of glucose metabolism in the frontal, parietal and temporal, but not occipital, lobes.[26]

A small case series of 4 patients with AD had previously reported no association between CCD and cortical accumulation of β-amyloid as imaged by ^{11}C-PIB,[25] which was confirmed in our cohort of 74 A + T+ patients. This supports the hypothesis that in subjects with AD, CCD is due to neurodegeneration that is unrelated to local amyloid pathology. This finding is in line with previous reports on neurodegeneration in AD being related to topographical distribution of tau more strongly than β-amyloid.[32,33,73–76] The fact that in our cohort, the relationship between tau and CCD was mediated by cortical hypometabolism in A + T+ subjects suggests that tau pathology drives the diaschisis in AD. This is not surprising, given the known relationship between topographical distribution of ^{18}F-Flortaucipir and neurodegeneration.[32,33,75,76] The absence of an association between tau and CCD in β-amyloid negative patients further supports this hypothesis, since in most cases these subjects present negligible or very mild ^{18}F-Flortaucipir binding in the cortex compared to AD patients.[55]

The lack of association between the cerebellar IA of ^{18}F-FDG, ^{18}F-Flortaucipir and ^{11}C-PIB in our biomarker-confirmed AD patients supports the hypothesis that cerebellar asymmetry of glucose metabolism is truly reflecting diaschisis from supratentorial involvement rather than contribution from local AD pathology. We cannot exclude, however, local factors that may play a role in some specific cases, such as in subjects with advanced disease or autosomal dominant AD, since amyloid does accumulate in the cerebellum in very late stages of the disease,[77] even leading to increased signal on ^{11}C-PIB in very rare cases.[78,79] Furthermore, it is known that persistent CCD can be associated with irreversible degeneration[6,10] and even atrophy perceptible on structural imaging in severe cases.[80,81] This may explain recent findings of a higher rate of cerebellar atrophy in Alzheimer's disease and frontotemporal dementia.[82,83]

Finally, regarding the clinical significance of CCD, in stroke, some studies have suggested an association of CCD with stroke severity, infarct volume and worse clinical outcome. However, Pappata et al. found no clinical correlates,[84] hence, prognostic value and clinical significance of this phenomenon remain controversial.[6,7,11,43–45,57,85] In glioma, CCD was shown to be associated with shorter survival.[46] Similar to the correlation between the degree of CCD and clinical scale of stroke severity demonstrated by Szilagyi et al.,[86] we found that cerebellar IA on ^{18}F-FDG showed a weak correlation with clinical measures of dementia severity. Although the p values were statistically significant for these associations, the small r^2 values suggest that these correlations may not be clinically meaningful. Furthermore, our mediation analysis suggests that this association is primarily driven by greater supratentorial asymmetry in patients with more severe disease. Larger longitudinal studies would be needed to investigate the relationship between CCD, disease progression and cognition.[83,87–89] The presence of CCD did not seem to impact cerebellar function as measured on neurological exam in our patient cohort, although the retrospective nature of this study limits the validity of these findings, especially our sensitivity to identify clinical correlates.

One technical consideration arising from our results is that supratentorial neurodegeneration can have a functional impact on cerebellar metabolism and therefore affect uptake in a cerebellar ROI. This should be considered when choosing a reference region for PET processing, as previously suggested by other authors.[83] Similarly, abnormalities in cerebellar metabolism, even in the absence of frank asymmetry, should be considered during clinical interpretation of FDG PET scans, especially when considering the cerebellum as a "reference" for evaluation of supratentorial activity.

The present study has several limitations. Although the patient cohort was large (n = 197) compared to previous reports of CCD in neurodegenerative conditions, the relationship between ^{18}F-FDG, ^{11}C-PIB and ^{18}F-Flortaucipir could only be studied in a relatively limited number of participants (n = 74). In addition, the relationship between proteinopathies underlying non-AD disorders (such as non-AD tauopathies, TDP-43, FUS) and CCD could not be assessed since no PET tracer is currently available to measure non-AD proteinopathies. Furthermore, our cohort is a convenience sample that is not representative of a typical clinical population given the relatively young mean patient age and high prevalence of atypical Alzheimer's disease phenotypes and non-AD disorders. The current findings, therefore, may not be generalizable to older, more

typical AD populations. We must also recognize that the present study did not consider other causes of cerebellar hypometabolism, which, although rare, could cause false positive CCD on PET, such as cerebellar infarcts or other vascular lesions, spinocerebellar degeneration, ataxia syndromes, cerebellitis, and congenital malformations.[90–92] These cases, however, if presenting with isolated cerebellar asymmetry on ^{18}F-FDG in the absence of contralateral supratentorial asymmetry, would not be considered to have CCD according to our operational definition, and such abnormalities would be identified on visual inspection of structural MRI. Additional limitations include the interval between PET scans using all 3 tracers which was relatively long in some patients, although results did not change when restricting analyses to patients with an interval between scans of less than a month. Finally, the retrospective nature of the study led to variation in between scan intervals and missing data in some participants. For instance, tests of cerebellar function were assessed retrospectively in patients' charts and were not available in all subjects. Prospective studies with a more detailed assessment of cerebellar function would be pertinent.

In summary, CCD is common in patients with neurodegenerative syndromes, and is more prevalent with certain clinical phenotypes, especially those with typically asymmetric presentations such as CBS, svPPA and lvPPA. In patients with AD, as demonstrated by ^{11}C-PIB and ^{18}F-Flortaucipir, the association between cerebellar asymmetry on ^{18}F-FDG and cortical ^{18}F-Flortaucipir suggests a tau-related disruption of cortico-ponto-cerebellar pathways, while amyloid does not seem to play a direct role. Further studies are required to elucidate the prognostic value and clinical correlates of CCD.

Funding

The author(s) disclosed receipt of the following financial support for the research, authorship, and/or publication of this article: This study was supported by National Institute on Aging grants (R01-AG-045611 to G.D.R.; P30-AG062422 to B.L.M. and G.D.R.; P01-AG19724 to B.L.M, K99AG065501 to R.L.J.), Rainwater Charitable Foundation (Tau Consortium) (to G.D.R. and W.J.J.), the Alzheimer's Association (AARF-16-443577 to R.L.J.), State of California Department of Health Services Alzheimer's Disease Research Centre of California grant (04-33516 to B.L.M.) and a gift from Edward and Pearl Fein (to G.D.R.).

Acknowledgements

We would like to acknowledge all patients and caregivers for their time and participation in this study. Avid Radiopharmaceuticals enabled use of the precursor for ^{18}F-Flortaucipir but did not provide direct funding and was not involved in data analysis or interpretation.

Declaration of conflicting interests

The author(s) declared the following potential conflicts of interest with respect to the research, authorship, and/or publication of this article: **K.P., R.L.J., L.I., L.E., A.S., T.J.M., J.P., S.B.:** no financial disclosure, **B.M.L.:** In the past 2 years: Cambridge NIHR BRC, advisory committee, J Douglas French Alzheimer's Foundation, Board of Directors, The Bluefield Project for Frontotemporal Dementia Research, Medical Advisor and grant, Rainwater Charitable Foundation, consulting, Stanford Alzheimer's Disease Research Center, consulting, Buck Institute SAB, consulting, Larry L. Hillblom Foundation, consulting, University of Texas Center for Brain Health, education consulting, University of Washington Alzheimer's Disease Research, Center EAB, consulting, Harvard University Alzheimer's Disease Research Center EAB, consulting, Safely You, Board of Directors, Guilford Press, royalties, Cambridge University Press, royalties, Johns Hopkins Press, royalties, Oxford University Press, royalties, Neurocase, Editor, Frontiers in Neurology, Section Editor
W.J.J.: In past 2 years: consulting for Biogen, Grifols, Bioclinica, Genentech, Novartis, **G.D.R.:** Research support from Avid Radiopharmaceuticals, GE Healthcare, Life Molecular Imaging, Genentech, Roche. In the past 2 years: consulting for Axon Neurosciences, Eisai, Johnson & Johnson, Genentech, Roche. Associate Editor for JAMA Neurology.

Authors' contributions

K.P.: study conception and design, acquisition of data, analysis, interpretation, drafting and revision of manuscript; R.L.J.: study conception and design, acquisition of data, analysis, interpretation, drafting and revision of manuscript; A.S.: study conception and design, acquisition of data, analysis, interpretation, critical revision of manuscript; L.I.: study conception and design, data analysis, interpretation, critical revision of manuscript; L.E.: study conception and design, acquisition of data, analysis, interpretation, critical revision of manuscript; T.J.M.: acquisition of data, critical revision of manuscript; J.P.: acquisition of data, critical revision of manuscript; S.L.B.: data acquisition, analysis, critical revision of manuscript. B.L.M.: acquisition of data, critical revision of manuscript; W.J.J.: study conception and design, acquisition of data, interpretation, critical revision of manuscript; G.D.R.: study conception and design, acquisition of data, interpretation, critical revision of manuscript. All authors have approved the final version of the manuscript.

Supplementary material

Supplemental material for this article is available online.

ORCID iD

Karine Provost https://orcid.org/0000-0002-5311-6758

References

1. Baron JC, Bousser MG, Comar D, et al. "Crossed cerebellar diaschisis" in human supratentorial brain infarction. *Trans Am Neurol Assoc* 1981; 105: 459–461.
2. Baron JC, Rougemont D, Soussaline F, et al. Local interrelationships of cerebral oxygen consumption and glucose utilization in normal subjects and in ischemic stroke patients: a positron tomography study. *J Cereb Blood Flow Metab* 1984; 4: 140–149.
3. Pantano P, Baron JC, Samson Y, et al. Crossed cerebellar diaschisis. Further studies. *Brain* 1986; 109: 677–694.
4. Feeney DM and Baron JC. Diaschisis. *Stroke* 1986; 17: 817–830.
5. Gold L and Lauritzen M. Neuronal deactivation explains decreased cerebellar blood flow in response to focal cerebral ischemia or suppressed neocortical function. *Proc Natl Acad Sci USA* 2002; 99: 7699–7704.
6. Lewis DH, Toney LK and Baron JC. Nuclear medicine in cerebrovascular disease. *Semin Nucl Med* 2012; 42: 387–405.
7. Sommer WH, Bollwein C, Thierfelder KM, et al. Crossed cerebellar diaschisis in patients with acute middle cerebral artery infarction: occurrence and perfusion characteristics. *J Cereb Blood Flow Metab* 2016; 36: 743–754.
8. Kim SE, Choi CW, Yoon BW, et al. Crossed-cerebellar diaschisis in cerebral infarction: technetium-99m-HMPAO SPECT and MRI. *J Nucl Med* 1997; 38: 14–19.
9. Agrawal KL, Mittal BR, Bhattacharya A, et al. Crossed cerebellar diaschisis on F-18 FDG PET/CT. *Indian J Nucl Med* 2011; 26: 102–103.
10. Shih WJ, Huang WS and Milan PP. F-18 FDG PET demonstrates crossed cerebellar diaschisis 20 years after stroke. *Clin Nucl Med* 2006; 31: 259–261.
11. Sobesky J, Thiel A, Ghaemi M, et al. Crossed cerebellar diaschisis in acute human stroke: a PET study of serial changes and response to supratentorial reperfusion. *J Cereb Blood Flow Metab* 2005; 25: 1685–1691.
12. Miyazaki D, Fukushima K, Nakahara A, et al. Crossed cerebellar diaschisis in status epilepticus. *Intern Med* 2016; 55: 1649–1651.
13. Mewasingh LD, Christiaens F, Aeby A, et al. Crossed cerebellar diaschisis secondary to refractory frontal seizures in childhood. *Seizure* 2002; 11: 489–493.
14. Ferilli MAN, Brunetti V, Costantini EM, et al. Left hemispheric status epilepticus with crossed cerebellar diaschisis. *J Neurol Neurosurg Psychiatry* 2018; 89: 311–312.
15. Graffeo CS, Snyder KA, Nasr DM, et al. Prognostic and mechanistic factors characterizing seizure-associated crossed cerebellar diaschisis. *Neurocrit Care* 2016; 24: 258–263.
16. Cianfoni A, Luigetti M, Bradshaw ML, et al. MRI findings of crossed cerebellar diaschisis in a case of Rasmussen's encephalitis. *J Neurol* 2010; 257: 1748–1750.
17. Shetty-Alva N, Novotny EJ, Shetty T, et al. Positron emission tomography in Rasmussen's encephalitis. *Pediatr Neurol* 2007; 36: 112–114.
18. Thajeb P, Shih BF and Wu MC. Crossed cerebellar diaschisis in herpes simplex encephalitis. *Eur J Radiol* 2001; 38: 55–58.
19. Alavi A, Mirot A, Newberg A, et al. Fluorine-18-FDG evaluation of crossed cerebellar diaschisis in head injury. *J Nucl Med* 1997; 38: 1717–1720.
20. Teoh EJ, Green AL and Bradley KM. Crossed cerebellar diaschisis due to cerebral diffuse large B cell lymphoma on 18F-FDG PET/CT. *Int J Hematol* 2014; 100: 415–416.
21. Otte A, Roelcke U, von Ammon K, et al. Crossed cerebellar diaschisis and brain tumor biochemistry studied with positron emission tomography, [18F]fluorodeoxyglucose and [11C]methionine. *J Neurol Sci* 1998; 156: 73–77.
22. Kajimoto K, Oku N, Kimura Y, et al. Crossed cerebellar diaschisis: a positron emission tomography study with L-[methyl-11C]methionine and 2-deoxy-2-[18F]fluoro-D-glucose. *Ann Nucl Med* 2007; 21: 109–113.
23. Calabria F and Schillaci O. Recurrent glioma and crossed cerebellar diaschisis in a patient examined with 18F-DOPA and 18F-FDG PET/CT. *Clin Nucl Med* 2012; 37: 878–879.
24. Priftakis D, Rondogianni P and Datseris I. A case of crossed cerebellar diaschisis on follow-up positron emission tomography/computed tomography with ((18)F) fluoro-D-glucose after treatment for glioblastoma. *World J Nucl Med* 2019; 18: 71–73.
25. Reesink FE, Garcia DV, Sanchez-Catasus CA, et al. Crossed cerebellar diaschisis in alzheimer's disease. *Curr Alzheimer Res* 2018; 15: 1267–1275.
26. Akiyama H, Harrop R, McGeer PL, et al. Crossed cerebellar and uncrossed basal ganglia and thalamic diaschisis in Alzheimer's disease. *Neurology* 1989; 39: 541–548.
27. Al-Faham Z, Zein RK and Wong CY. 18F-FDG PET assessment of lewy body dementia with cerebellar diaschisis. *J Nucl Med Technol* 2014; 42: 306–307.
28. Wile D, Dhaliwal H, Sarna JR, et al. Diaschisis as the presenting feature in sporadic Creutzfeldt-Jakob disease. *JAMA Neurol* 2013; 70: 408–409.
29. Nishioka K, Suzuki M, Satoh K, et al. Crossed cerebellar diaschisis in Creutzfeldt-Jakob disease evaluated through single photon emission computed tomography. *J Neurol Sci* 2018; 395: 88–90.
30. Marquie M, Normandin MD, Vanderburg CR, et al. Validating novel tau positron emission tomography tracer [F-18]-AV-1451 (T807) on postmortem brain tissue. *Ann Neurol* 2015; 78: 787–800.
31. Bejanin A, Schonhaut DR, La Joie R, et al. Tau pathology and neurodegeneration contribute to cognitive impairment in Alzheimer's disease. *Brain* 2017; 140: 3286–3300.
32. Ossenkoppele R, Schonhaut DR, Scholl M, et al. Tau PET patterns mirror clinical and neuroanatomical variability in Alzheimer's disease. *Brain* 2016; 139: 1551–1567.
33. Iaccarino L, Tammewar G, Ayakta N, et al. Local and distant relationships between amyloid, tau and neurodegeneration in Alzheimer's disease. *Neuroimage Clin* 2018; 17: 452–464.
34. La JR, Visani AV, Baker SL, et al. Prospective longitudinal atrophy in Alzheimer's disease correlates with the

intensity and topography of baseline tau-PET. *Sci Transl Med* 2020; 12: 01–03.
35. Fung CW, Guo J, Fu H, et al. Atrophy associated with tau pathology precedes overt cell death in a mouse model of progressive tauopathy. *Sci Adv* 2020; 6: eabc8098.
36. Gordon BA, Blazey TM, Christensen J, et al. Tau PET in autosomal dominant Alzheimer's disease: relationship with cognition, dementia and other biomarkers. *Brain* 2019; 142: 1063–1076.
37. Xu G, Zheng S, Zhu Z, et al.; for the Alzheimer's Disease Neuroimaging Initiative. Association of tau accumulation and atrophy in mild cognitive impairment: a longitudinal study. *Ann Nucl Med* 2020; 34: 815–823.
38. Sintini I, Graff-Radford J, Senjem ML, et al. Longitudinal neuroimaging biomarkers differ across Alzheimer's disease phenotypes. *Brain* 2020; 143: 2281–2294.
39. La Joie R, Visani AV, Lesman-Segev OH, et al. Association of APOE4 and clinical variability in Alzheimer disease with the pattern of tau- and amyloid-PET. *Neurology* 2021; 96: e650–e661.
40. Berti V, Pupi A and Mosconi L. PET/CT in diagnosis of movement disorders. *Ann N Y Acad Sci* 2011; 1228: 93–108.
41. Spinelli EG, Mandelli ML, Miller ZA, et al. Typical and atypical pathology in primary progressive aphasia variants. *Ann Neurol* 2017; 81: 430–443.
42. Madhavan A, Whitwell JL, Weigand SD, et al. FDG PET and MRI in logopenic primary progressive aphasia versus dementia of the Alzheimer's type. *PLoS One* 2013; 8: e62471.
43. Infeld B, Davis SM, Lichtenstein M, et al. Crossed cerebellar diaschisis and brain recovery after stroke. *Stroke* 1995; 26: 90–95.
44. Serrati C, Marchal G, Rioux P, et al. Contralateral cerebellar hypometabolism: a predictor for stroke outcome? *J Neurol Neurosurg Psychiatry* 1994; 57: 174–179.
45. Takasawa M, Watanabe M, Yamamoto S, et al. Prognostic value of subacute crossed cerebellar diaschisis: single-photon emission CT study in patients with Middle cerebral artery territory infarct. *AJNR Am J Neuroradiol* 2002; 23: 189–193.
46. Segtnan EA, Grupe P, Jarden JO, et al. Prognostic implications of total hemispheric glucose metabolism ratio in cerebrocerebellar diaschisis. *J Nucl Med* 2017; 58: 768–773.
47. Kramer JH, Jurik J, Sha SJ, et al. Distinctive neuropsychological patterns in frontotemporal dementia, semantic dementia, and Alzheimer disease. *Cogn Behav Neurol* 2003; 16: 211–218.
48. Albert MS, DeKosky ST, Dickson D, et al. The diagnosis of mild cognitive impairment due to Alzheimer's disease: recommendations from the national institute on Aging-Alzheimer's association workgroups on diagnostic guidelines for Alzheimer's disease. *Alzheimers Dement* 2011; 7: 270–279.
49. McKhann GM, Knopman DS, Chertkow H, et al. The diagnosis of dementia due to Alzheimer's disease: recommendations from the National Institute on Aging-Alzheimer's Association workgroups on diagnostic guidelines for Alzheimer's disease. *Alzheimers Dement* 2011; 7: 263–269.
50. Rascovsky K, Hodges JR, Knopman D, et al. Sensitivity of revised diagnostic criteria for the behavioural variant of frontotemporal dementia. *Brain* 2011; 134: 2456–2477.
51. Gorno-Tempini ML, Hillis AE, Weintraub S, et al. Classification of primary progressive aphasia and its variants. *Neurology* 2011; 76: 1006–1014.
52. Armstrong MJ, Litvan I, Lang AE, et al. Criteria for the diagnosis of corticobasal degeneration. *Neurology* 2013; 80: 496–503.
53. Litvan I, Agid Y, Calne D, et al. Clinical research criteria for the diagnosis of progressive supranuclear palsy (Steele-Richardson-Olszewski syndrome): report of the NINDS-SPSP international workshop. *Neurology* 1996; 47: 1–9.
54. Maass A, Landau S, Baker SL, et al.; Alzheimer's Disease Neuroimaging Initiative. Comparison of multiple tau-PET measures as biomarkers in aging and Alzheimer's disease. *Neuroimage* 2017; 157: 448–463.
55. Tsai RM, Bejanin A, Lesman-Segev O, et al. 18)F-flortaucipir (AV-1451) tau PET in frontotemporal dementia syndromes. *Alzheimers Res Ther* 2019; 11: 13–02.
56. Baker SL, Maass A and Jagust WJ. Considerations and code for partial volume correcting [(18)F]-AV-1451 tau PET data. *Data Brief* 2017; 15: 648–657.
57. Liu Y, Karonen JO, Nuutinen J, et al. Crossed cerebellar diaschisis in acute ischemic stroke: a study with serial SPECT and MRI. *J Cereb Blood Flow Metab* 2007; 27: 1724–1732.
58. Jack CR, Jr., Bennett DA, Blennow K, et al. A/T/N: an unbiased descriptive classification scheme for Alzheimer disease biomarkers. *Neurology* 2016; 87: 539–547.
59. Rabinovici GD, Rosen HJ, Alkalay A, et al. Amyloid vs FDG-PET in the differential diagnosis of AD and FTLD. *Neurology* 2011; 77: 2034–2042.
60. Ossenkoppele R, Rabinovici GD, Smith R, et al. Discriminative accuracy of [18F]flortaucipir positron emission tomography for Alzheimer disease vs other neurodegenerative disorders. *Jama* 2018; 320: 1151–1162.
61. Baker SL, Harrison TM, Maass A, et al. Effect of off-target binding on (18)F-Flortaucipir variability in healthy controls across the lifespan. *J Nucl Med* 2019; 60: 1444–1417.
62. Choi JY, Cho H, Ahn SJ, et al. Off-Target (18)F-AV-1451 binding in the basal ganglia correlates with Age-Related iron accumulation. *J Nucl Med* 2018; 59: 117–120.
63. project Tj. jamovi (Version 1.2). *Computer Software* 2020.
64. Crutch SJ, Schott JM, Rabinovici GD, et al.; Alzheimer's Association ISTAART Atypical Alzheimer's Disease and Associated Syndromes Professional Interest Area. Consensus classification of posterior cortical atrophy. *Alzheimers Dement* 2017; 13: 870–884.
65. Bevan Jones WR, Cope TE, Passamonti L, et al. [(18)F] AV-1451 PET in behavioral variant frontotemporal dementia due to MAPT mutation. *Ann Clin Transl Neurol* 2016; 3: 940–947.

66. Bevan-Jones WR, Cope TE, Jones PS, et al. [(18)F]AV-1451 binding in vivo mirrors the expected distribution of TDP-43 pathology in the semantic variant of primary progressive aphasia. *J Neurol Neurosurg Psychiatry* 2018; 89: 1032–1037.
67. Tetzloff KA, Graff-Radford J, Martin PR, et al. Regional distribution, asymmetry, and clinical correlates of tau uptake on [18F]AV-1451 PET in atypical Alzheimer's disease. *J Alzheimers Dis* 2018; 62: 1713–1724.
68. Scholl M, Damian A and Engler H. Fluorodeoxyglucose PET in neurology and psychiatry. *PET Clin* 2014; 9: 371–390.
69. Matias-Guiu JA, Diaz-Alvarez J, Ayala JL, et al. Clustering analysis of FDG-PET imaging in primary progressive aphasia. *Front Aging Neurosci* 2018; 10: 230–208.
70. Forster A, Kerl HU, Goerlitz J, et al. Crossed cerebellar diaschisis in acute isolated thalamic infarction detected by dynamic susceptibility contrast perfusion MRI. *PLoS One* 2014; 9: e88044.
71. Martin WR and Raichle ME. Cerebellar blood flow and metabolism in cerebral hemisphere infarction. *Ann Neurol* 1983; 14: 168–176.
72. Poretti A and Boltshauser E. Crossed cerebro-cerebellar diaschisis. *Neuropediatrics* 2012; 43: 53–54.
73. Ossenkoppele R, Schonhaut DR, Baker SL, et al. Tau, amyloid, and hypometabolism in a patient with posterior cortical atrophy. *Ann Neurol* 2015; 77: 338–342.
74. Brier MR, Gordon B, Friedrichsen K, et al. Tau and Abeta imaging, CSF measures, and cognition in Alzheimer's disease. *Sci Transl Med* 2016; 8: 338ra366.
75. Cho H, Choi JY, Hwang MS, et al. Tau PET in alzheimer disease and mild cognitive impairment. *Neurology* 2016; 87: 375–383.
76. Xia C, Makaretz SJ, Caso C, et al. Association of in vivo [18F]AV-1451 tau PET imaging results with cortical atrophy and symptoms in typical and atypical Alzheimer disease. *JAMA Neurol* 2017; 74: 427–436.
77. Thal DR, Rub U, Orantes M, et al. Phases of a beta-deposition in the human brain and its relevance for the development of AD. *Neurology* 2002; 58: 1791–1800.
78. Knight WD, Okello AA, Ryan NS, et al. Carbon-11-Pittsburgh compound B positron emission tomography imaging of amyloid deposition in presenilin 1 mutation carriers. *Brain* 2011; 134: 293–300.
79. La Joie R, Ayakta N, Seeley WW, et al. Multisite study of the relationships between antemortem [(11)C]PIB-PET centiloid values and postmortem measures of Alzheimer's disease neuropathology. *Alzheimers Dement* 2019; 15: 205–216.
80. Mahale R, Mehta A and Rangasetty S. Crossed cerebellar diaschisis due to Rasmussen encephalitis. *Pediatr Neurol* 2015; 53: 272–273.
81. Tien RD and Ashdown BC. Crossed cerebellar diaschisis and crossed cerebellar atrophy: correlation of MR findings, clinical symptoms, and supratentorial diseases in 26 patients. *AJR Am J Roentgenol* 1992; 158: 1155–1159.
82. Tabatabaei-Jafari H, Walsh E, Shaw ME, et al.; Alzheimer's Disease Neuroimaging Initiative (ADNI). The cerebellum shrinks faster than normal ageing in Alzheimer's disease but not in mild cognitive impairment. *Hum Brain Mapp* 2017; 38: 3141–3150.
83. Guo CC, Tan R, Hodges JR, et al. Network-selective vulnerability of the human cerebellum to Alzheimer's disease and frontotemporal dementia. *Brain* 2016; 139: 1527–1538.
84. Pappata S, Mazoyer B, Tran Dinh S, et al. Effects of capsular or thalamic stroke on metabolism in the cortex and cerebellum: a positron tomography study. *Stroke* 1990; 21: 519–524.
85. Laloux P, Meurisse H and de Coster P. Crossed cerebellar hypoperfusion in mesencephalic infarcts. *Clin Nucl Med* 1997; 22: 399–400.
86. Szilagyi G, Vas A, Kerenyi L, et al. Correlation between crossed cerebellar diaschisis and clinical neurological scales. *Acta Neurol Scand* 2012; 125: 373–381.
87. Rapoport M, van Reekum R and Mayberg H. The role of the cerebellum in cognition and behavior: a selective review. *J Neuropsychiatry Clin Neurosci* 2000; 12: 193–198.
88. Buckner RL, Krienen FM, Castellanos A, et al. The organization of the human cerebellum estimated by intrinsic functional connectivity. *J Neurophysiol* 2011; 106: 2322–2345.
89. Schmahmann JD. From movement to thought: anatomic substrates of the cerebellar contribution to cognitive processing. *Hum Brain Mapp* 1996; 4: 174–198.
90. Shih WJ and Schleenbaker RE. Asymmetrical cerebellar uptake in brain single photon emission computed tomography. *Semin Nucl Med* 1992; 22: 51–53.
91. Vella A and Mascalchi M. Nuclear medicine of the cerebellum. In: Manto M and Huisman TAGM (eds) *Handbook of clinical neurology*. 3rd series ed. Amsterdam: Elsevier, 2018, pp.251–266.
92. Oh M, Kim JS, Oh JS, et al. Different subregional metabolism patterns in patients with cerebellar ataxia by 18F-fluorodeoxyglucose positron emission tomography. *PLoS One* 2017; 12: e0173275.